Citation for published version:
Malfense Fierro, G-P & Meo, M 2019, 'Bolt assessment of wind turbine hub using nonlinear ultrasound methods', *Wind Engineering*. https://doi.org/10.1177/0309524X19887739

DOI:
10.1177/0309524X19887739

Publication date:
2019

Document Version
Peer reviewed version

Link to publication

Bolt assessment of wind turbine hub using nonlinear ultrasound methods

Gian Piero Malfense Fierro and Michele Meo
University of Bath, Materials Research, Department of Mechanical Engineering, Claverton Down, Bath, UK

Abstract

This work evaluates various nonlinear ultrasound methods for *in-situ* structural health monitoring (SHM) of the loosened state of a four bolt structure found on large scale wind turbines The aim was assessment of a four bolted structure with only two piezoelectric sensors and determination of individual bolt loosened and the extent of loosening. Nonlinear ultrasound methods have been shown to have advantages over linear methods in terms of sensitive, although the detection accuracy and robustness of these methods can be highly dependent on correct frequency selection. Thus, a frequency selection process based on the modal response of the structure is suggested for determination of bolt specific frequencies, which was then used to evaluate the individual bolt loosened state. Two nonlinear ultrasound techniques were used to evaluate the bolted structure; the 2^{nd} and 3^{rd} order nonlinearity parameters and a nonlinear acoustic moment's method. The modal response method used for frequency selection was able to determine specific bolt frequencies based on surface and bolt velocities. Nonlinear evaluation at these frequencies showed that specific frequencies related to individual bolts and as the bolts loosened there was a clear increase in the production of nonlinearities. Thus the loosened status of individual bolts could be tracked using specific pre-identified frequencies.

Keywords: Wind Turbine, Ultrasound, Nonlinear Ultrasound, Structural Health Monitoring, Bolted Structure, Sparse Array

1.1. Introduction

The Global Wind Energy Council presented the sixth edition of the Global Wind Energy Outlook (2016) which outlined some of the main issues facing wind energy as well as growth areas. The industry has seen growth of around 17% in 2015, with over 433GW installed. It is expected that installed wind power will exceed 888GW by 2025, thus showing the potential of the market and the large amount of maintenance that would be needed for the hundreds of wind farms [1]. The cost of maintenance and catastrophic failure mechanisms present in wind turbines highlight the importance of reliable *in-situ* SHM systems. Some of these costs have been discussed by Ciang, Lee and Bang 2008 [2] and include difficulties to perform inspection and maintenance work due to the ever growing sizes of wind turbines, human costs such as fatal accidents, locations of wind turbines (usually remote and difficult to get to), difficulties in setting up equipment due to location or terrain and the increase in wind turbine sizes and price.

Hameed, Hong, Cho, Ahn and Song 2009 [3] discusses some of the main SHM advantages for wind turbines which include early warning (which avoids breakdown and repair costs), problem identification (allows for the right service at the right time, ultimately reducing the maintenance costs) and continuous monitoring (providing constant information that the system is working). Due to the complexity of wind turbines there are multiple possible failure mechanisms from generators and electrical system failures to mechanical failures of rotor blades and hubs. Germanischer 2007 [4] identifies that these failures can be attributed to many different defects within the system such as: surface damages, cracks, structural discontinuities, damage to lightning protection systems, leakages, corrosion, wear, fastenings, and dirt to name a few.

The gigantic size of modern wind turbines (diameters of between 40m and 90m) emphasise the importance of the joint, as failure would be catastrophic. Khan, Iqbal and Khan 2005 [5] suggests that bolt failure and reliability to be the fourth worst after blade tip breaking, yaw bearing failure and blade failures. There is a multitude of different techniques available to assess the structural integrity of wind turbines although most of the methods used to date focus on blade and tower failure. The various testing techniques employed have been summarised by Ciang, Lee and Bang 2008 [2] and include: acoustic emissions, thermal imaging, ultrasonic, modal approaches, Laser Vibrometery, and electric resistance among others.

Bolted joints are usually made up of bolts, washers and nuts that are used to apply a preload to the joint. The washers are used to distribute load in a clamped member while the nut allows for the disassembly of the joint. Preloading of the bolt can be simply described by a series of springs: where k_b refers to the bolt stiffness and k_m refers to the members' stiffness. In a joint with two bolted components this can be described as two in-line springs with the same or different stiffness (depending on material of the member). Typically joints are designed to result in bolt failure this is done as the bolts are not expensive and easily replaced. Evaluation of the loosened state of the bolt can have large implications on structural health monitoring (SHM) of joints, as current maintenance programs are systematically carried out. The development of *in-situ* systems with the ability to assess individual as well as group bolt states would advance the monitoring of structures incorporating bolted joints.

This work looks to assess the ability of two nonlinear ultrasound techniques (second/third order nonlinearity parameters and nonlinear acoustic moments) to determine the loosened state of a bolted structure. If a single bolted structure is considered and the bolt loosens, a reduction in stiffness is expected and thus changes in the bolt state can be evaluated by damping or amplitude changes. Considering, a multi-bolted structure, the reduction in the clamp load and stiffness of one bolt plays a smaller and smaller role in overall stiffness. This generally results in difficulty of linear methods to effectively evaluate these small changes when considering an *in-situ* SHM approach. Assessment of the loosened state is thus generally achieved by monitoring each bolt individually with a consequent increase in cost. An *in-situ* method able to detect bolt loosening with a minimum number of transducers/sensors would improve safety and reduce maintenance cost as long as accuracy and reliability are improved or maintained.

Recently, there has been an increased focus on nonlinear ultrasound techniques as they have been found to be more sensitive than linear methods [6-8] and therefore in the case of a loaded structure the sensitivity of these methods may result in advantages in evaluation [9]. Many nonlinear ultrasofund techniques have been developed over the years, which have focused on; detection and localisation of structural defects such as micro-cracks (fatigue) [10, 11], delaminations [12, 13], weak adhesive bonds and others [14, 15], nonlinear elastic wave spectroscopy (NEWS) [16-18], nonlinear elastic wave modulation [19-23] and nonlinear imaging techniques [24-29].

Works relating to bolted structures include: subharmonic resonance for detection of bolt joint looseness [30], hybrid higher order harmonic and spectral sideband for continuous monitoring of bolt loosening [31] and nonlinear crack-wave interactions [32]. The vast amount of research has shown relationships between a wide array of nonlinear harmonic generation (subharmonic, higher harmonics and modulated harmonics) and the loosened state of bolted structures, while also evaluating various nonlinear modelling approaches (classic and non-classical nonlinearities). Acoustic moment methods have been used to evaluate the health of adhesive joints and bonds [33-36]. Although, these studies do not generally consider the difficulty and importance of correct frequency selection when considering nonlinear techniques. Due to the relative low amplitude (and signal to noise ratio) of nonlinearities generated by interfaces, it is vital that these signal amplitudes are improved.

The structure investigated in this work is a simple representation of a bolted structure tasked with joining the turbine blades to the hub on large wind turbines. Generally, turbine hubs are circular structures with multiple bolts (up to 100s) which allow for the blades to be connected using multiple bolts, the structure used in this work provides a steel structure with multiple bolt locations to simulate part of the actual structure (refer to Figure 1 below). Depending on the size of the turbine bolt, torque requirements range from hundreds of Nm for M24 (~600Nm) bolts to thousands of Nm for M36 (~3000Nm), with these values varying depending no design considerations. In this work M24 bolts were spaced 75mm apart and were used up to a maximum torque of 350Nm, in order to simulate individual bolt loosening. A generic solution is provided in this work that can then be applied to various hub and bolt layouts.

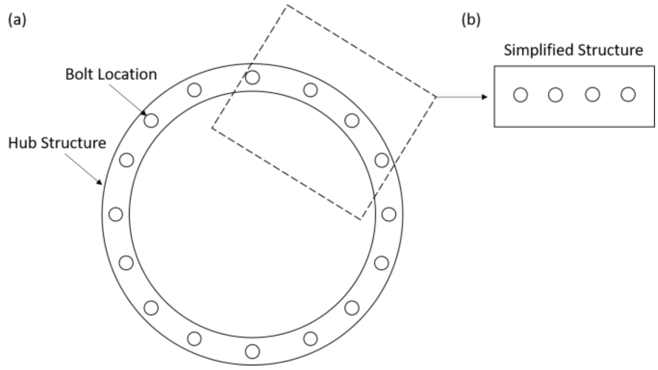

Figure 1: Generic hub layout (a) and simplified hub layout (b)

The structure evaluated can be described as a simple tension joint consisting of two identical steel bolted parts consisting of four bolts, and can be assumed to be a simple representation of a section of a circular hub. The ability to detect individual bolt loosening would have great significance in improving maintenance and monitoring of such structures. Thus, the main aim of the experiment was to assess the loosened state of each of the four bolts with only two ultrasound piezoelectric transducers (PZTs).
Experimentation was conducted by fastening bolts at predetermined levels of torque (clamping force) using a torque wrench. This tightening of the bolt follows a defined sequence of events and causes predictable results in the fastener. If the nut and head of the bolt are firmly seated against non-compressible materials the torsional action of tightening the assembly stretches the bolts, thus creating tension in the bolt. Preloading in most cases is required to make the fastening and the build-up of tension can be controlled by the torque applied. This tensile pre-stress (equivalent to the compressive stress introduced in the joint material) which is determined by the levels of torque the bolts are tightened with have large implications on the behaviour and life of the joint. Some of the issues that can affect tension joints over time are if the bolts are clamped with too little force loosening may occur. Whereas if the bolts are clamped with too much force (the proof load of the bolt may be exceeded) leading to failure, warping, advancement of hydrogen embrittlement and stress corrosion cracking.
Considering the applications of nonlinear methods it is expected that as the clamping force increases, the load or pressure between the two connected surfaces of the joint will increase along with the load or pressure between the bolt head/nut, washer and top surface. It is also expected that this increase in pressure will have an opposite effect on the production of the nonlinear parameters, which is that there should be a decrease in these parameters as torque is applied to the system. The modal velocities of the structure at various resonance frequencies were determined in order to evaluate whether individual bolts could be excited by specific frequencies. Frequency selection based on these modal responses was then used to evaluate the nonlinear responses of the structure, with the aim of identifying which bolt had loosened.

1.2. Related Theory

1.2.1. Experimental Second and Third Order Nonlinearity Parameters

Nonlinear ultrasound techniques and methods centre on the theory of the ‘clapping/rubbing’ mechanism, which include cracks and debonded surfaces. When an ultrasonic signal passes through a crack the propagation of the wave forces the crack to open and close, this opening and closing gives rise to further harmonics in the response signal. These further harmonics are known as the second harmonic, third harmonic and so forth. Nonlinear ultrasound uses these extra harmonics to determine the extent of defects in a material. Figure 2 below shows the further harmonics that are produced for single-frequency. Figure 2 highlights the second ($2f1$) and third ($3f1$) harmonics produced from a single frequency ($f1$) signal.

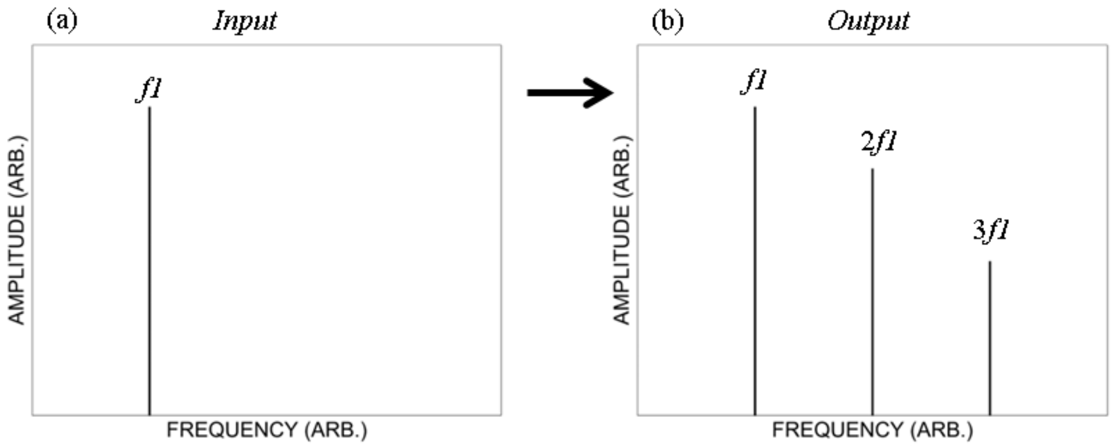

Figure 2: Plot (a) shows the input signal for a single frequency, plot (b) shows the output signals for a single frequency.

The development of the theory behind nonlinear ultrasonic methods has been well documented and tested. The fundamental equations used and developed in order to determine the further harmonics (second and third order nonlinearity parameters) are highlighted below. These equations provide essential information that allow for these harmonics to be quantified and analysed. The second order nonlinearity parameters can be described by the equation below.[37]:

$$\beta = \frac{8A_2}{A_1^2 k^2 a_1}$$

Eq. (1.1)

Where: A_1 and A_2 are the respective frequency amplitudes of the first and second harmonics of the recorded time domain waveforms, k is the wavenumber, and a_1 is the propagation distance.
The third order nonlinearity parameter is shown below [38]:

$$\gamma \approx \frac{48A_3}{A_1 k^3 a_1}$$

Eq. (1.2)

Where: A_3 is the frequency amplitude of the third harmonic of the recorded time domain waveform.

1.2.2. Nonlinear Acoustic Moment evaluation

Previous studies using acoustic moments have focused mainly on the health of adhesive joints and bonds. This work focuses on developing a methodology that uses both the linear and nonlinear acoustic moments of a given signal to help determine the loosened state of bolts present in a compression loaded specimen.
The nonlinear acoustic moment of an output signal in the frequency domain is measured by evaluating the power spectral density (PSD) or the power of the signal. The PSD function evaluates the power (V^2/Hz) of a signal over a specific frequency range, this is then integrated to determine the energy of the signal in terms of time. The nonlinear acoustic moment requires that the energy of each frequency response be calculated. The fundamental frequency is the initial driving frequency and the second and third harmonics are two and three times the fundamental frequency, respectively. The Power Spectral Density and Acoustic Moment can be defined as [39]:

$$W(f) = Y.conj(Y)/L$$

Eq. (1.3)

$$M_n = \int_0^{f_N} W(f) f^n df$$

Eq. (1.4)

Where: W(f) is the Power Spectral Density (PSD) function, Y is the Fast Fourier transform (FFT) of the time domain series, L is the length of the time domain series, f is the frequency variable, f_N is the Nyquist frequency.

The zeroth moment or M_0 means the signal energy calculated as the area under the spectral density curve, and can be analytically related to the mean square of voltage signals [39]. The M_0 mode is described by the following function:

$$M_0 = \int_0^{f_N} W(f)df$$

Eq. (1.5)

The acoustic moment for the individual frequency band (i.e. 20kHz) can be described as:

$$M_f = \int_{fl}^{fh} W(f)df$$

Eq. (1.6)

Where: f is the frequency assessed, fh is a point just after the frequency band, and fl is a point just before the frequency band.

The individual frequency spikes (in the frequency domain) were examined and the individual acoustic moments were assessed. For example Figure 3 shows the selection of the frequency band (highlighted in red) that would be used to determine the acoustic moment. Any noise below fl and above fh is filtered out, thus by integrating between fh and fl it is possible to measure the acoustic moment for that particular frequency (this can be applied to the fundamental frequency as well as the further harmonics second and third). This method allows for direct comparison between the linear acoustic moment (calculated from the fundamental frequency, i.e. 10kHz) and the nonlinear acoustic moments (calculated from the second and third harmonics generated by a loosening of the contact interface, i.e. 20kHz and 30kHz respectively).

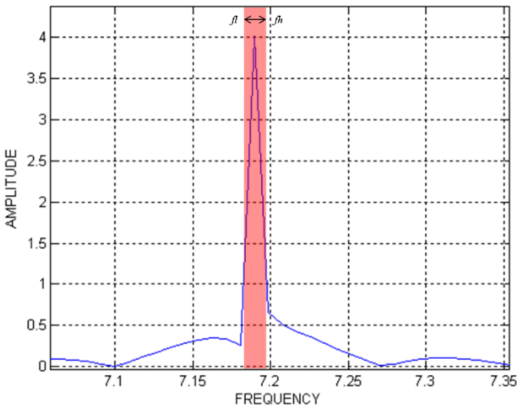

Figure 3: Acoustic Moment Band Selection (7.19kHz)

The nonlinear acoustic moments refer to moments of the second and third harmonic, while the linear acoustic moment refers to the moment of the fundamental frequency. The results were evaluated by examining the ratio of the nonlinear moments over the linear moment. Remembering that the specific frequency bands were individually selected and the acoustic moment determined for each band, the following ratios were used to evaluate the effect of loading in the structure and are described below.

The Second Harmonic Acoustic Moment Ratio:

$$\delta_{f2/f1} = \frac{M_{f2}}{M_{f1}}$$

Eq. (1.7)

Third Harmonic Acoustic Moment Ratio:

$$\delta_{f3/f1} = \frac{M_{f3}}{M_{f1}}$$

Eq. (1.8)

Second and Third Harmonic Acoustic Moment Ratio:

$$\delta_{(f2+f3)/f1} = \frac{M_{f2}+M_{f3}}{M_{f1}}$$

Eq. (1.9)

Where: M_{f2} is the moment of the second harmonic, M_{f3} the moment of the third harmonic, M_{f1} is the moment of the fundamental frequency, δ is the ratio of the respective moments. These ratios were used to evaluate the structure at different loads and at the above described frequencies.

The acoustic moment ratios were evaluated for various bolt loading conditions for a compression loaded structure which allowed comparison of the parameter as bolts loosened.

There is an inverse relationship between the linear and nonlinear acoustic moments which is related to the transfer of energy from the excitation frequency (linear response) into higher harmonics (nonlinear response). In a system with forced excitation there is a finite level of energy, excitation of interfaces (such as those found in a bolted structure) can result in the generation of contact nonlinearities due to the 'clapping or rubbing' of these interfaces. Thus, the theoretical expectation is that as loading increases the linear acoustic moment should increase (less energy loss to defected or debonded regions), while the nonlinear acoustic moment should decrease as less energy is converted into higher harmonics at contact interfaces due to improved contact and loading of the structure. As load is decreased in the system, contact nonlinearities are generated at interfaces, which result in the conversion of energy from the fundamental excitation frequency into higher harmonics (multiples of the fundamental), hence an inverse relationship.

The inverse relationship between the linear acoustic moment and the nonlinear acoustic moments should allow for a good contrast in behaviour and thus good sensitivity in terms of structural loading changes. Acoustic moment methods rely on determining the signal energy and how this energy is affected by damage or load.

1.3. Experimental Setup

The bolted structure evaluated consisted of two identical steel rectangular blocks (345mm x 200mm, with a depth of 100mm) fastened by four bolts (M24) (Figure 4, Figure 5), and used eight washers. The bolts were located central in terms of the vertical plane (100mm up), and 60mm from either side with 75mm between each bolt. A TTi 50MHz Function Generator (Arbitrary and Pulse) TG5011 was used to generate the output signal, while a Falco Systems DC-5MHz High Voltage Amplifier WMA-300 was used to amplifier the output signal. A Picoscope 4424 was used as the oscilloscope to capture and process the output signal on a laptop. Four PZTs were used to evaluate the specimen: PZT 1 was a Panametrics NDT 100kHz actuator, PZT 2 was a Panametrics 0.5MHz and used to capture the output signal, while PZT 3 and PZT 4 were both APC International PZTs (Diameter 6.35mm, Thickness 0.25mm, Type 850 WFB). PZT 1 and 2 were located in two different locations L1 (top surface on opposite corners) (Figure 4 and Figure 5) and L2 (middle of the two blocks on the front and back surface Figure 5) which allowed for a transmission test through the thickness.

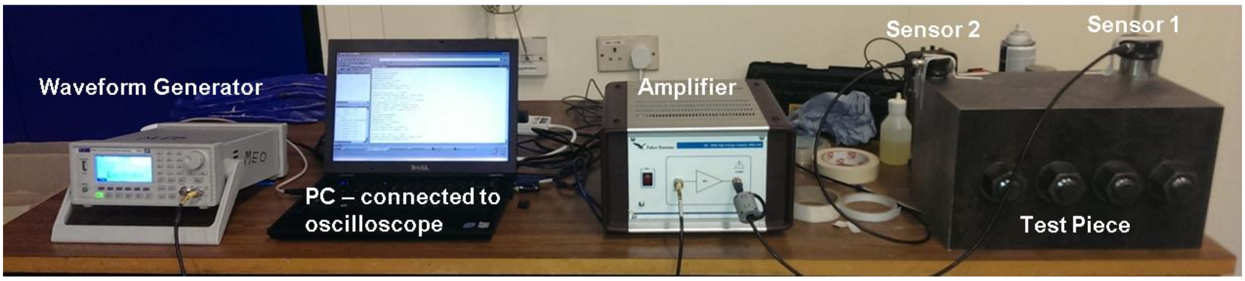

Figure 4: Experiment Setup

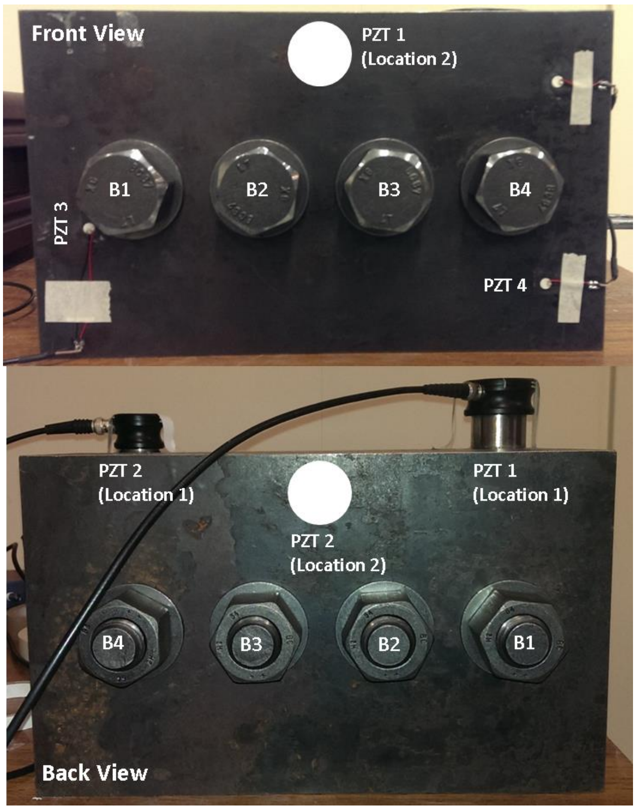

Figure 5: Test Piece: PZTs and Bolt Locations

Five cases were used to evaluate the looseness of the bolts, shown below in Table 1 and Table 2. While Figure 6 shows the side view of the structure in two loading conditions (Figure 6(b) and (d)), determined by increasing preloading (tightening) of the bolts. It is expected that as load increases the nonlinear responses (β, γ, $\delta_{f2/f1}$, $\delta_{f3/f1}$ and $\delta_{(f2+f3)/f1}$) should decrease (Figure 6(e)). The excitation method used a single frequency wave (Figure 6(a)) to excite the structure, which was determined by evaluating the resonance frequencies of the bolted structure.

Different fastening cases	
CASE 0 (C0)	All bolts (B1, B2, B3, B4) are fastened.
CASE 1 (C1)	B1 is gradually unfastened, while B2, B3, B4 remain fastened.
CASE 2 (C2)	B2 is gradually unfastened, while B1, B3, B4 remain fastened.
CASE 3 (C3)	B3 is gradually unfastened, while B1, B2, B4 remain fastened.
CASE 4 (C4)	B4 is gradually unfastened, while B1, B2, B3 remain fastened.
CASE 5 (C5)	All bolts are unfastened gradually by the same amount.

Table 1: Different fastening cases.

	Applied torque for bolts- PZT 1 & 2 (L1)	**Applied torque for bolts- PZT 1 & 2 (L2)**	**Applied torque for bolts- PZT 3 & 4**
C0	350Nm	250Nm	350Nm

C1	B2, B3, B4 = 350Nm B1 reduced: 350, 300, 250, 200, 150	B2, B3, B4 = 250Nm B1 reduced: 250, 200 150, 100, 50, 0	B2, B3, B4 = 350Nm B1 reduced: 350, 250, 150, 0
C2	B1, B3, B4 = 350Nm B2 reduced: 350, 300, 250, 200, 150	B1, B3, B4 = 250Nm B2 reduced: 250, 200 150, 100, 50, 0	B1, B3, B4 = 350Nm B2 reduced: 350, 250, 150, 0
C3	B1, B2, B4 = 350Nm B3 reduced: 350, 300, 250, 200, 150	B1, B2, B4 = 250Nm B3 reduced: 250, 200 150, 100, 50, 0	B1, B2, B4 = 350Nm B3 reduced: 350, 250, 150, 0
C4	B1, B2, B3 = 350Nm B4 reduced: 350, 300, 250, 200, 150	B1, B2, B3 = 250Nm B4 reduced: 250, 200 150, 100, 50, 0	B1, B2, B3 = 350Nm B4 reduced: 350, 250, 150, 0
C5	350, 250, 150, 0		350, 250, 150, 0

Table 2: Torque Strategies

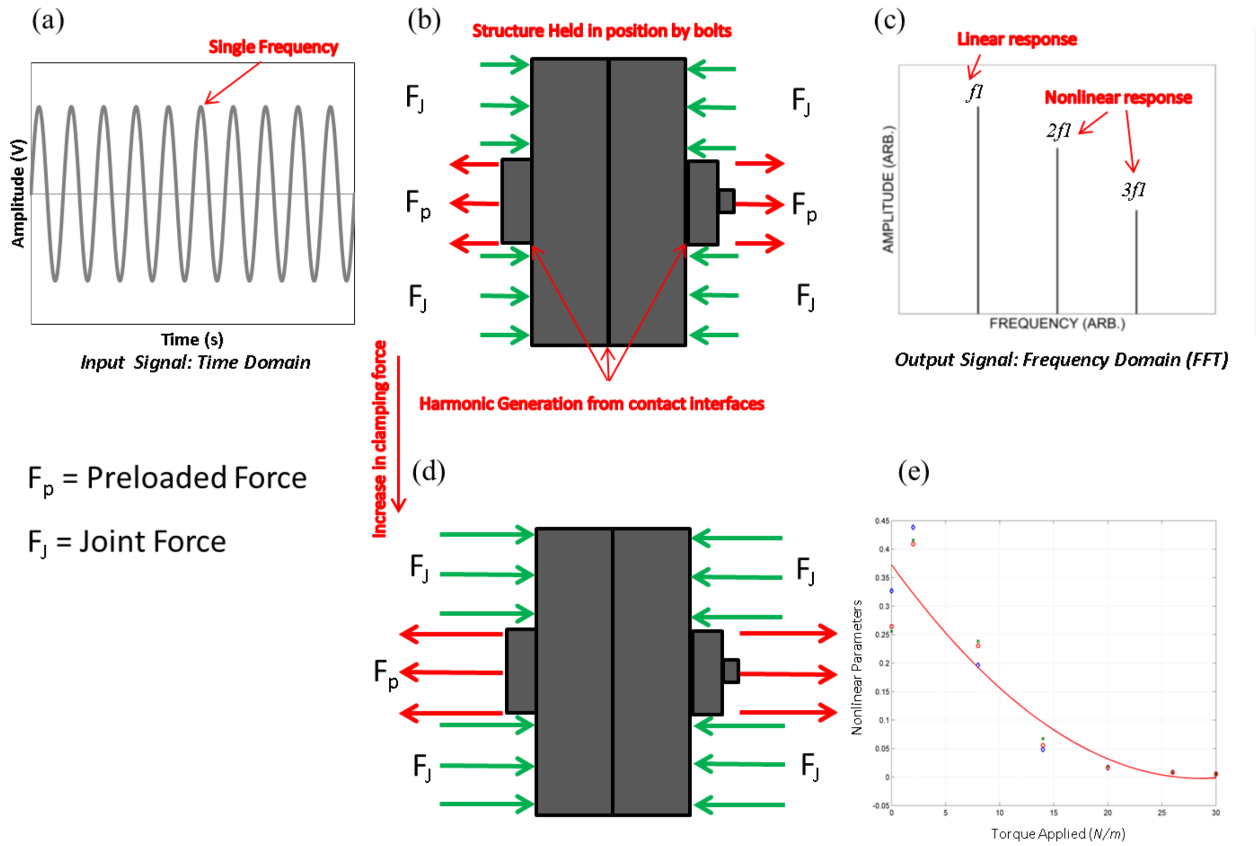

Figure 6: Single frequency input signal (a), force diagram of bolted structure (b), nonlinear responses (c), increase in clamping force of bolted structure (d), and expected nonlinear response of system vs. torque (e).

The structure was excited using a sweep function of the waveform generator in order to determine the resonance frequencies of the structure, observed as the peaks (Figure 7 and Table 3 below). After which a Laser Vibrometer was used to measure surface and bolt modal velocities.

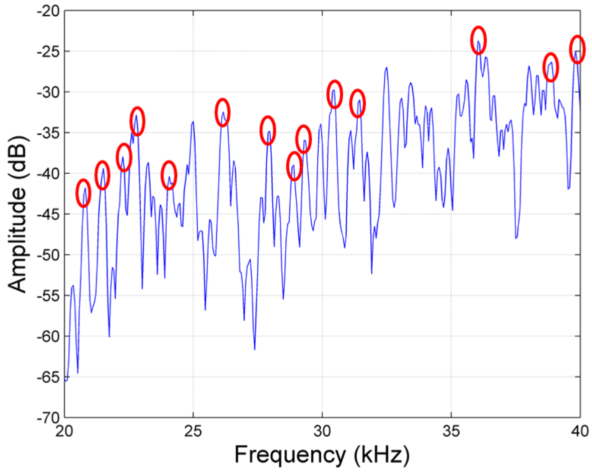

Figure 7: Frequency Sweep between 20kHz and 40kHz

Resonance Frequencies (kHz)
5.300, 6.900,7.800, 9.090, 10.500, 10.640, 11.300, 11.600, 12.700, 13.250, 14.550, 15.200, 16.040, 17.550, 17.750, 18.100, 18.700, 19.500, 20.800, 21.500, 22.260, 22.800, 24.000, 26.160, 27.900, 28.900, 29.300, 30.450, 32.500, 36.050, 38.000, 39.850

Table 3: Resonance Frequencies

1.4. Modal Analysis and Results (β for PZTs 1 & 2 (L1))

A modal analysis method was investigated in order to evaluate its potential to determine which bolt had loosened. The structure was excited at the various resonance frequencies and the modal response of the individual bolts as well as the surface of the structure was measured using a Laser Vibrometer (LV). By assessing which bolt/surface modal velocities were greatest at the various bolt locations and for the various frequencies tested, it was assumed that for a bolt in position 1 where modal displacements are maximised in that area alone at a given frequency the response should be the greatest for that bolt location. As torque decreases the nonlinear response for that bolt location should increase, while decreases occur at different bolt locations at the same frequency nothing specific should be observed. Thus by determining these individual bolt location frequencies it should be possible to pinpoint the loosened location. Nonlinear responses refer to second and third order nonlinear parameters as well as the nonlinear acoustic moments of the system.
A grid was setup using the LV to capture the out-of-plane velocity of the surface and bolt heads of the structure. Once the individual points had been evaluated an image was created using the LV software, which shows the velocity (fast Fourier transform (FFT) of data) of the points at the various frequencies. Four frequencies were tested to evaluate whether a bolt specific frequency could be determined, the frequencies tested were 21.5 kHz (B1 and C1), 20.8 kHz (B2 and C2), 24 kHz (B3 and C3) and 5.3 kHz (B4 and C4). It is expected that when the structure is excited at 21.5 kHz and all the various cases (1-4) are tested (as shown in Table 2) bolt 1 (B1) will give the greatest nonlinear parameter response as it is loosened.
As can be seen in Figure 8 below the velocity of B1 is far greater than those exhibited by the other bolts, suggesting: that at 21.5kHz it is possible to excite B1 to a greater extent than the other bolts. The hypothesis is that as the B1 becomes looser this movement relative to the other bolts will result in a greater generation of nonlinear responses due to the larger clapping mechanisms and by evaluating multiple frequencies it should be possible to determine frequencies that relate to individual bolt clapping mechanisms, ultimately allowing for individual bolt analysis of a structure.
The second-order nonlinearity parameter (β) was evaluated for 4 different bolt cases (C1, C2, C3 and C4, as described in Table 1 and Table 2 above), and it can clearly be seen that the nonlinear response for C1 (Figure 8(b)) increases as torque is reduced (reduction in clamping load at B1). The response for the other three cases (C2, B2 loosened only, C3, B3 loosened only and C4, B4 loosened only) show a

low relative response when compared to C1 as torque is reduced and no clear trend. The response of C2-C4, is due to the fact that 21.5kHz does not result in the production of high contact nonlinearities at these locations.

The final magnitude for C1 (at 150 Nm torque) is three times that of the next closest case and the nonlinear parameter β only exhibits a clear increasing trend when B1 is loosened and the structure excited at 21.5 kHz. The same approach was conducted for the other three cases and the results have been highlighted in Figure 9 to Figure 11.

(a) (b)

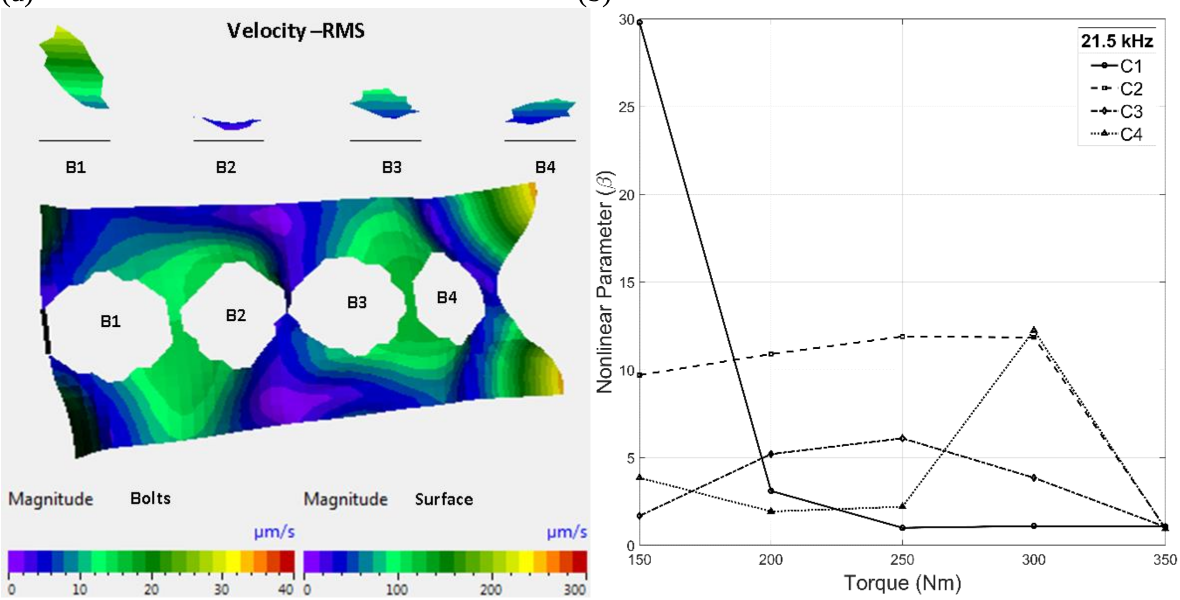

Figure 8: Out-of-plane velocity for the surface and bolts (a), second order nonlinear response (β) for four cases explored (21.5kHz, PZTs 1 & 2)

Figure 9 shows the modal and nonlinear results for 20.8kHz for the four investigated cases. The importance of the interaction of the bolts and surface to create clapping is underlined in this case as the velocities of the bolts suggest that C1 should give the best results. Although the surface velocities do not coincide with the bolts movements, with high displacement areas starting from the left side of B2 to the right side of B4, suggesting that B2, B3 and B4 should result in the greatest clapping regions. The magnitude of the surface response in most cases evaluated is generally much larger than the bolt response, suggesting that it is the main contributing factor in determining the correct bolt excitation. Good positive results are generated for C2 and C4, which are considered to be due to the larger magnitudes of surface velocities when compared to bolt velocities. While it was expected that C3, would provide good results at this frequency, it should be noted that B3 had a much tighter fit within the structure than the other bolts and thus provided lower generation of harmonics and in this case was not sufficiently excited.

(a) (b)

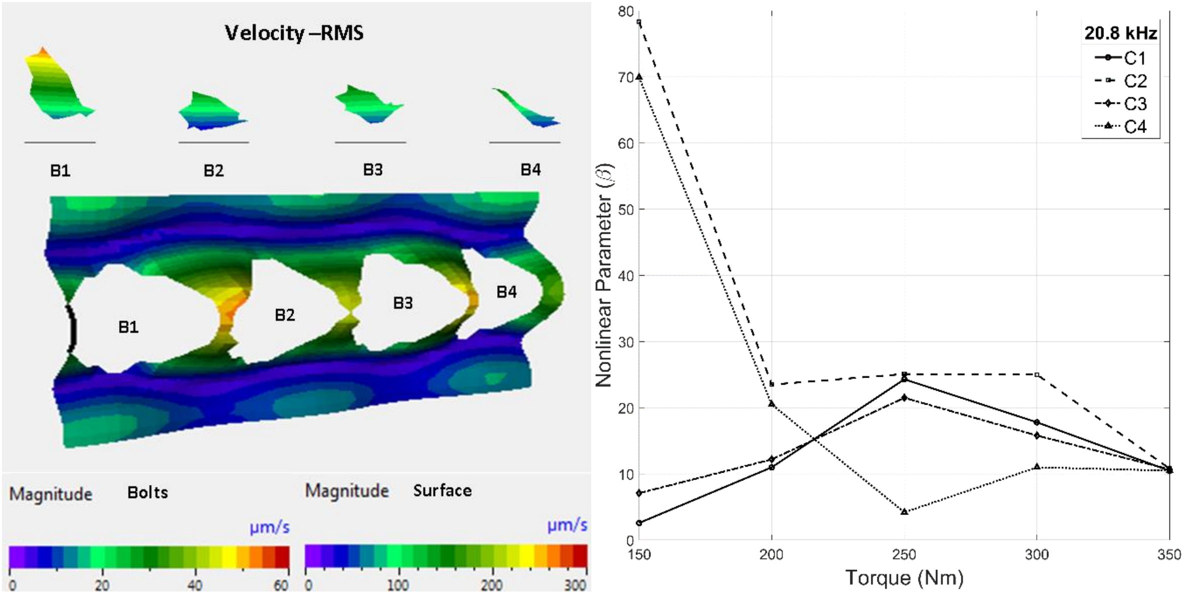

Figure 9: Out-of-plane velocity for the surface and bolts (a), second order nonlinear response (β) for four cases explored (20.8 kHz, PZTs 1 & 2)

Figure 10 follow from results found at 20.8kHz which suggest that surface displacements may be the main contributing factor to the generation of further harmonics due to the larger magnitude exhibited over the bolts in these cases. Bolt velocities suggest B1 should result in the best nonlinear response although B3 has the second greatest bolt velocity and there are more areas of high velocity surrounding B3 (on the surface: north east, south east and west – highest surface velocity near bolt) than compared with B1 (fewer areas and lower in amplitude).

(a) (b)

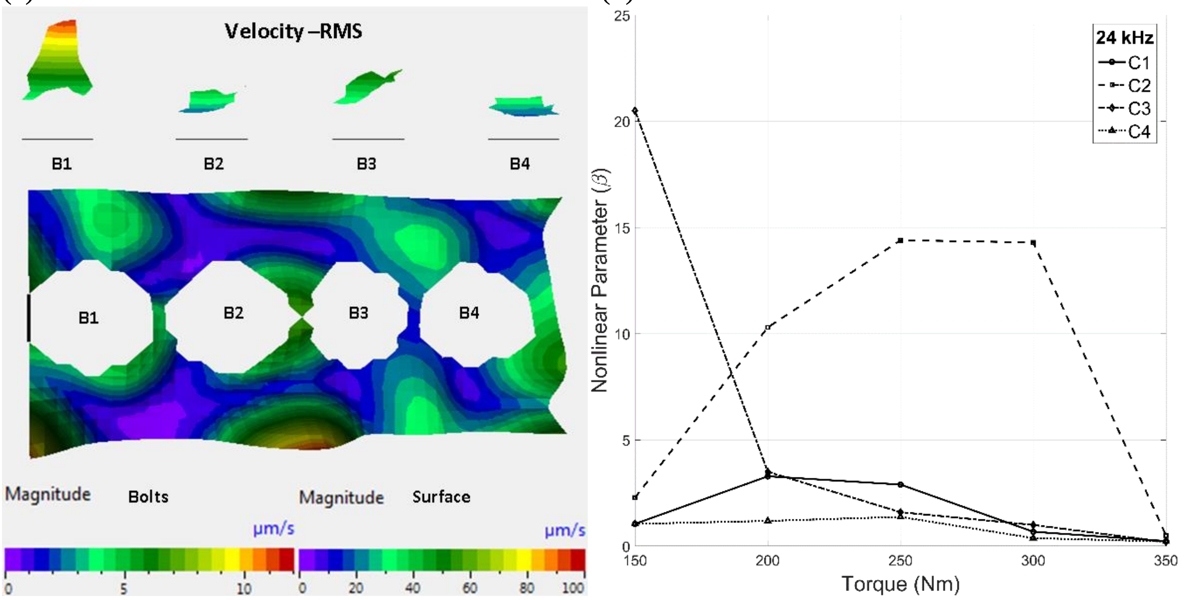

Figure 10: Out-of-plane velocity for the surface and bolts (a), second order nonlinear response (β) for four cases explored (24 kHz, PZTs 1 & 2)

Comparing the different cases (Figure 10 (b)) it was found that C3 had a clear trend and its final β magnitude was far greater than for the other cases.

Finally, Figure 11 shows the results for 5.3kHz, although in this case the difference in surface and bolt displacements are much lower than those found in the other cases. C4 exhibits a clear trend like in the other cases relating to other bolts.

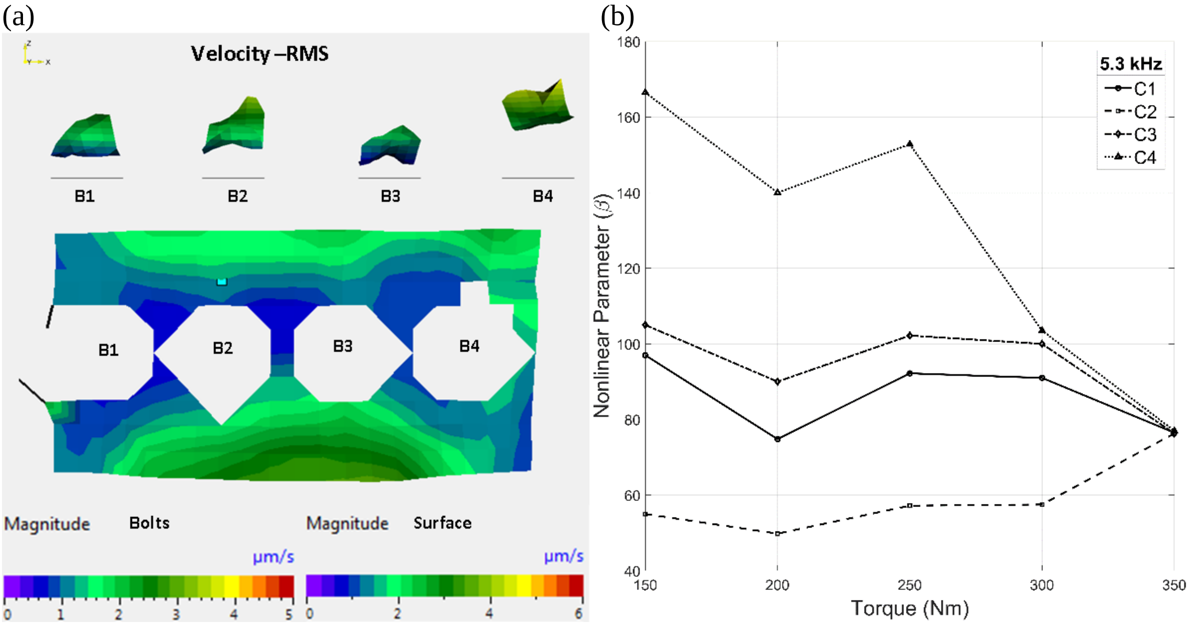

Figure 11: Out-of-plane velocity for the surface and bolts (a), second order nonlinear response (β) for four cases explored (5.3 kHz, PZTs 1 & 2).

Figure 8 to Figure 11 show that bolt specific frequencies can be determined by evaluating the interaction between the bolts and surface of the structure. Furthermore, it is possible to determine which bolt has loosened when considering the nonlinear parameter β. There is a clear correlation between the inherent clapping mechanisms within the structure, the torque applied and the modal velocity of the structure. Figure 12 shows results for multiple frequencies and for each bolt condition. Figure 12 highlights that multiple frequencies can be determine for each bolt with the values of β showing a clear increasing trend as torque decreases. In most cases there is at least a 100% increase in β as torque is reduced to 150 Nm from 350 Nm, and in some cases an order of magnitude increase, highlighting the sensitivity of β and methodology.

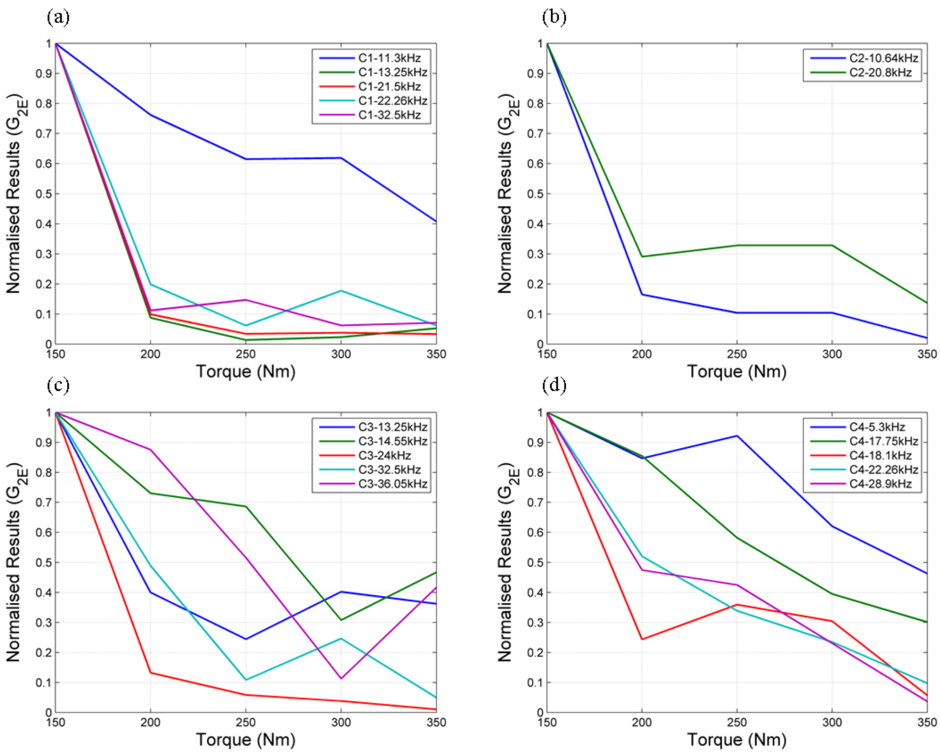

Figure 12: Normalised β results for various frequencies

Figure 13 below shows the flow chart highlighting the experimental methodology.

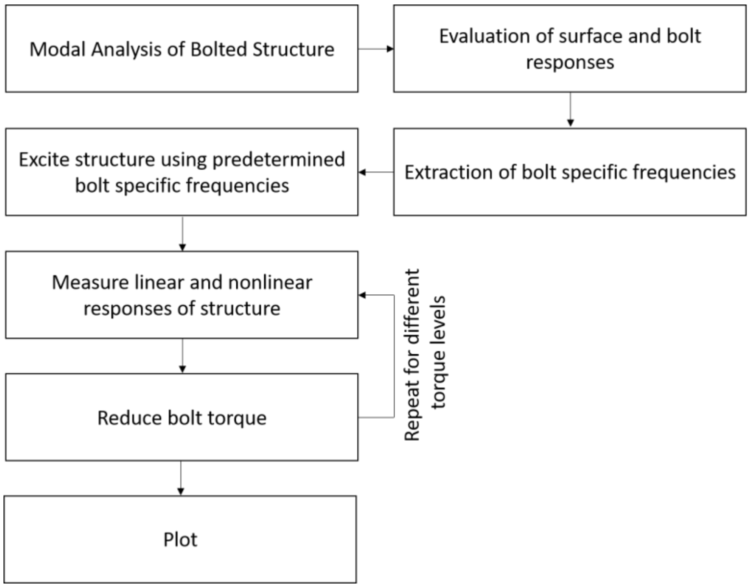

Figure 13: Flow chart of experimental methodology

1.4.1. Results: γ, $\delta_{f2/f1}$ and $\delta_{(f2+f3)/f1}$ for PZTs 1 & 2 (L1 and L2), β and γ for PZTs 3 & 4

The third order nonlinearity parameter (γ) and the nonlinear acoustic moments ($\delta_{f2/f1}$ and $\delta_{(f2+f3)/f1}$) were assessed for the PZTs 1 and 2 (Figure 14 and Figure 15), and the second and third order nonlinearity parameters (β and γ) for PZTs 3 and 4 (Figure 16). Please note max values have been normalised to 1. Generally, γ, $\delta_{f2/f1}$ and $\delta_{(f2+f3)/f1}$ follow the same trends as were found in the previous section, with increasing nonlinear parameters as torque was decreased for each of the bolt specific frequencies. It is expected that the γ figures should be similar to β as the governing nonlinear responses should generate a third harmonic as long as long as the response is large enough. In this case β was much greater than γ (by a factor of 3 orders of magnitude) due to the low relative response of the third harmonic. Generally, results for γ and $\delta_{(f2+f3)/f1}$ were increasing versus decreases in torque.
Examining results from PZTs 3 & 4 (Figure 16) showed that similar trends were found in terms of bolt specific frequencies. Although after examining all the results not all the bolt frequency combinations found for PZTs 1 & 2 aligned with those found for the different PZTs and locations. Out of these frequencies, 21.5 kHz (B1, C1) and 5.3 kHz (B4, C4) produced good results, while B2 and B3 responded well to different frequencies (32.5 kHz and 29.3 kHz).
Important factors that are difficult to predict or quantify are which contact surface generate the greatest level of harmonics (contact between the bolted surfaces or between washer bolt head and surfaces) and whether the areas of production of these harmonics change as the bolts become looser. PZT 1 and 2, location 2, explored the effects of the contact surface of the two steel blocks by conducting a transmission test through the specimen. The results (Figure 15 and Figure 17) did show an increase in the nonlinear parameters as was expected even though fewer frequencies were found that exhibited this behaviour. The findings suggest that the contact condition between the two surfaces may not be greatly affected by the loosening of one bolt (which is expected) and the majority of clapping may in fact be attributed to the surface, washer and bolt. Another issue is the energy required to excite through the thickness of the structure, which may lead to the results in L2. Figure 17 shows the normalised results found by PZT 1 and 2 in location 2.

(a) (b)

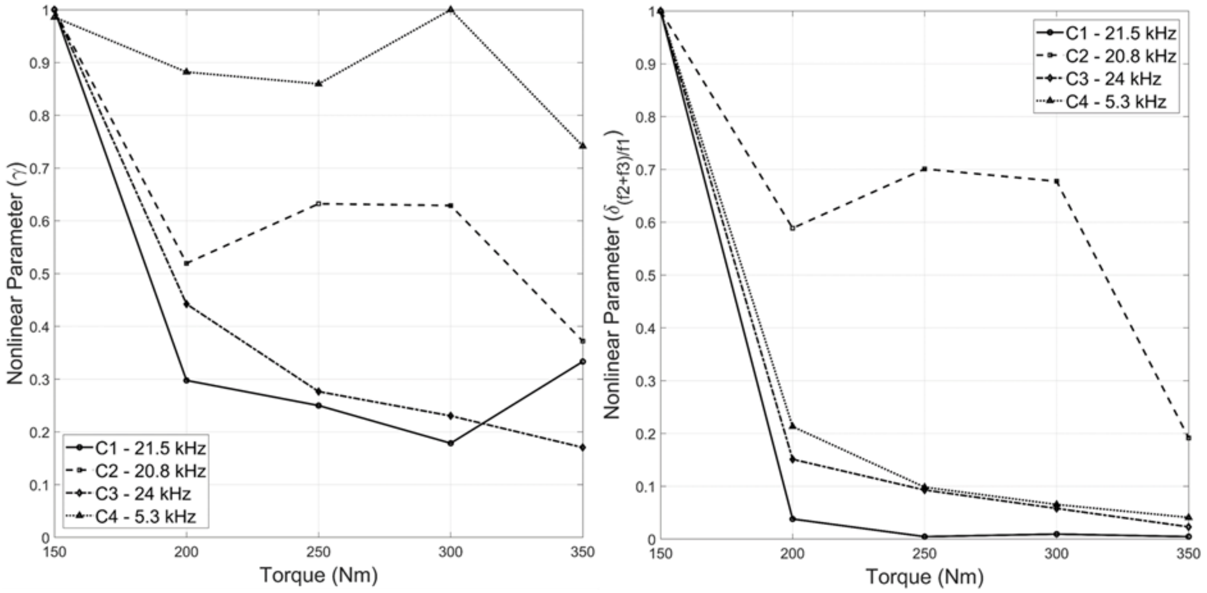

Figure 14: γ (a) and $\delta_{(f2+f3)/f1}$ (b) results for C1 to C4 (PZTs 1 & 2, L1)

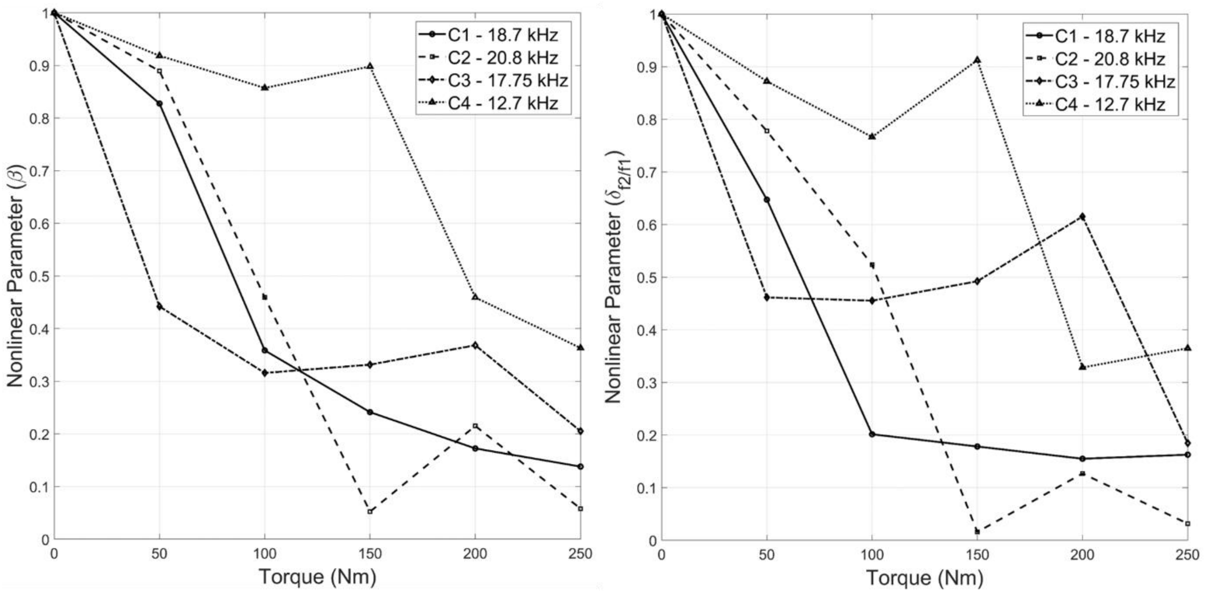

Figure 15: β (a) and $\delta_{f2/f1}$ (b) results for C1 to C4 (PZTs 1 & 2, L2)

(a) (b)

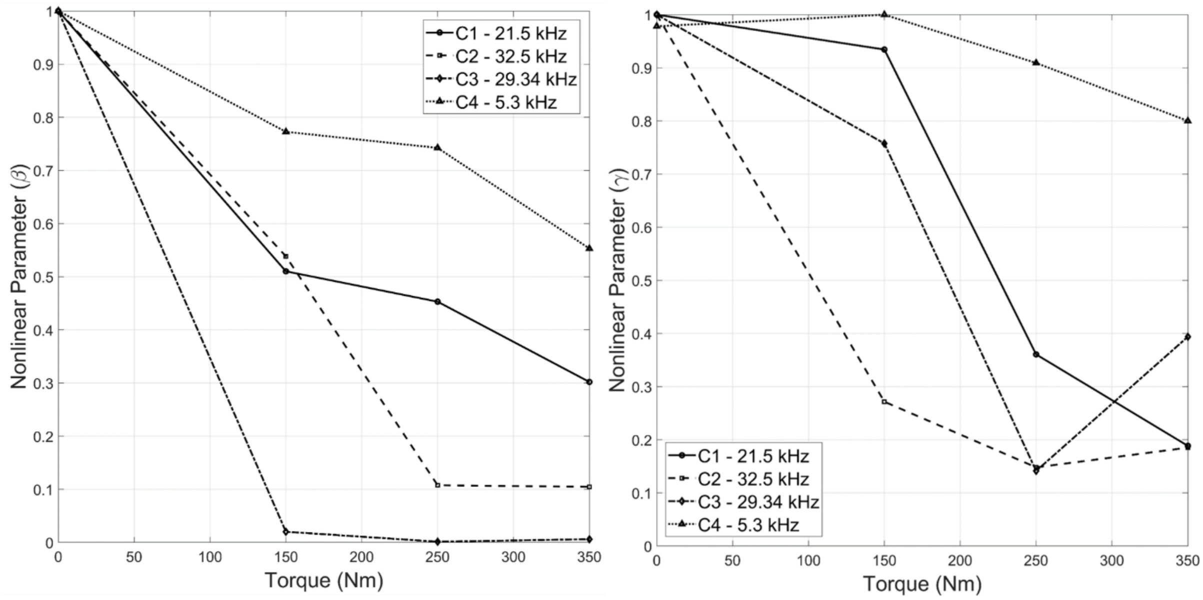

Figure 16: β (a) and γ (b) for C1 to C4 (PZTs 3 & 4)

(a) (b)

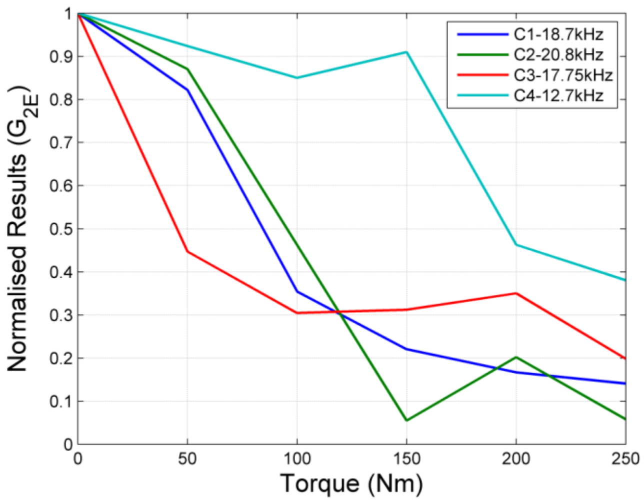

Figure 17: Normalised β Results for PZTs 1 and 2 (L2)

1.5. Conclusion

Two nonlinear ultrasound techniques were used to evaluate a wind turbine bolted structure; the 2nd and 3rd order nonlinearity parameters and a nonlinear acoustic moment's method. The nonlinear techniques used were coupled with a frequency selection process that relied on the modal response of the structure. A laser vibrometer was used to determine which frequencies provided the highest velocity near specific bolt locations, from which specific bolt frequencies were determined allowing for individual bolt assessment. After determining these specific frequencies, four nonlinear parameters (β, γ, $\delta_{f2/f1}$ and $\delta_{(f2+f3)/f1}$) from multiple PZT locations were used to evaluate the loosened state of the structure. The results showed that the nonlinear techniques were able to assess the individual bolt loosened state using the various evaluation techniques. Furthermore, the nonlinear parameters showed a clear increasing trend as individual bolts were loosened. The findings imply that clapping and generation of further harmonics are likely to come from surface interactions with the washers, bolt head and nut, and that these interactions can be estimated by evaluating the mode shape of the structure at different frequencies.

References:

[1] Fried, L., Shukla, S., Sawyer, S. and Teske, S., Global wind outlook 2016, (2016).

[2] Ciang, C. C., Lee, J.-R. and Bang, H.-J., Structural health monitoring for a wind turbine system: a review of damage detection methods, *Measurement Science and Technology* **19**, pp. 122001 (2008).

[3] Hameed, Z., Hong, Y., Cho, Y., Ahn, S. and Song, C., Condition monitoring and fault detection of wind turbines and related algorithms: A review, *Renewable and Sustainable energy reviews* **13**, pp. 1-39 (2009).

[4] Germanischer, L., Wind Energy, GL Wind.“, *Possible Wind Turbine Damage* **30**, (2007).

[5] Khan, M. M., Iqbal, M. T. and Khan, F., Electrical and Computer Engineering, 2005. Canadian Conference on, IEEE, pp. 1978-1981.(2005)

[6] Cantrell, J. H. and Yost, W. T., Nonlinear ultrasonic characterization of fatigue microstructures, *International Journal of fatigue* **23**, pp. 487-490 (2001).

[7] Boccardi, S., CALLA, D., FIERRO, G.-P., Ciampa, F. and Meo, M., Nonlinear Damage Detection and Localisation Using a Time Domain Approach, *Structural Health Monitoring 2015*, (2015).

[8] Fierro, G. P. M. and Meo, M., Nonlinear imaging (NIM) of flaws in a complex composite stiffened panel using a constructive nonlinear array (CNA) technique, *Ultrasonics* **74**, pp. 30-47 (2017).

[9] Fierro, G.-P. M. and Meo, M., 9th International Conference on Composite Science And Technology.(2013)

[10] Dziedziech, K., Pieczonka, L., Adamczyk, M., Klepka, A. and Staszewski, W. J., Efficient swept sine chirp excitation in the non-linear vibro-acoustic wave modulation technique used for damage detection, *Structural Health Monitoring*, pp. 1475921717704638 (2017).

[11] Sohn, H., Lim, H. J., DeSimio, M. P., Brown, K. and Derriso, M., Nonlinear ultrasonic wave modulation for online fatigue crack detection, *Journal of Sound and Vibration* **333**, pp. 1473-1484 (2014).

[12] Klepka, A., Pieczonka, L., Staszewski, W. and Aymerich, F., Impact damage detection in laminated composites by non-linear vibro-acoustic wave modulations, *Composites Part B: Engineering* **65**, pp. 99-108 (2014).

[13] Delrue, S., Tabatabaeipour, M., Hettler, J. and van Den Abeele, K., Non-destructive evaluation of kissing bonds using local defect resonance (LDR) spectroscopy: a simulation study, *Physics Procedia* **70**, pp. 648-651 (2015).

[14] Ulrich, T., Johnson, P. A. and Guyer, R. A., Interaction dynamics of elastic waves with a complex nonlinear scatterer through the use of a time reversal mirror, *Physical review letters* **98**, pp. 104301 (2007).

[15] Guyer, R. A. and Johnson, P. A., Nonlinear mesoscopic elasticity: Evidence for a new class of materials, *Physics today* **52**, pp. 30-36 (1999).

[16] Meo, M. and Zumpano, G., Nonlinear elastic wave spectroscopy identification of impact damage on a sandwich plate, *Composite structures* **71**, pp. 469-474 (2005).

[17] Ciampa, F., Pickering, S., Scarselli, G. and Meo, M., Health Monitoring of Structural and Biological Systems 2014, International Society for Optics and Photonics, pp. 906402.(2014)

[18] Scalerandi, M., Gliozzi, A., Bruno, C. L. E., Masera, D. and Bocca, P., A scaling method to enhance detection of a nonlinear elastic response, *Applied Physics Letters* **92**, pp. 101912 (2008).

[19] Straka, L., Yagodzinskyy, Y., Landa, M. and Hänninen, H., Detection of structural damage of aluminum alloy 6082 using elastic wave modulation spectroscopy, *NDT & E International* **41**, pp. 554-563 (2008).

[20] Fierro, G. P. M. and Meo, M., Residual fatigue life estimation using a nonlinear ultrasound modulation method, *Smart Materials and Structures* **24**, pp. 025040 (2015).

[21] Van Den Abeele, K.-A., Johnson, P. A. and Sutin, A., Nonlinear elastic wave spectroscopy (NEWS) techniques to discern material damage, part I: nonlinear wave modulation spectroscopy (NWMS), *Journal of Research in Nondestructive Evaluation* **12**, pp. 17-30 (2000).

[22] FIERRO, G. P. M. and MEO, M., Identification of the Location and Level of Loosening in a Multi-bolt Structure using Nonlinear Ultrasound, *Structural Health Monitoring 2017*, (2017).

[23] Fierro, G. P. M. and Meo, M., IWSHM 2017: Structural health monitoring of the loosening in a multi-bolt structure using linear and modulated nonlinear ultrasound acoustic moments approach, *Structural Health Monitoring* **17**, pp. 1349-1364 (2018).

[24] Dionysopoulos, D., Fierro, G. P. M., Meo, M. and Ciampa, F., Imaging of barely visible impact damage on a composite panel using nonlinear wave modulation thermography, *NDT & E International*, (2018).

[25] Fierro, G.-P. M., Pinto, F., Iacono, S. D., Martone, A., Amendola, E. and Meo, M., Monitoring of self-healing composites: a nonlinear ultrasound approach, *Smart Materials and Structures* **26**, pp. 115015 (2017).

[26] Fierro, G. P. M. and Meo, M., A combined linear and nonlinear ultrasound time-domain approach for impact damage detection in composite structures using a constructive nonlinear array technique, *Ultrasonics* **93**, pp. 43-62 (2019).

[27] Fierro, G. P. M. and Meo, M., Nonlinear Elastic imaging of barely visible impact damage in composite structures using a constructive nonlinear array sweep technique, *Ultrasonics*, (2018).

[28] Haupert, S., Renaud, G. and Schumm, A., Ultrasonic imaging of nonlinear scatterers buried in a medium, *NDT & E International* **87**, pp. 1-6 (2017).

[29] Solodov, I., Bai, J., Bekgulyan, S. and Busse, G., 18th World Conference on Nondestructive Testing, Citeseer, pp. 16-20.(2012)

[30] Zhang, M., Shen, Y., Xiao, L. and Qu, W., Application of subharmonic resonance for the detection of bolted joint looseness, *Nonlinear Dynamics* **88**, pp. 1643-1653 (2017).

[31] Zhang, Z., Liu, M., Liao, Y., Su, Z. and Xiao, Y., Contact acoustic nonlinearity (CAN)-based continuous monitoring of bolt loosening: Hybrid use of high-order harmonics and spectral sidebands, *Mechanical Systems and Signal Processing* **103**, pp. 280-294 (2018).

[32] Broda, D., Staszewski, W., Martowicz, A., Uhl, T. and Silberschmidt, V., Modelling of nonlinear crack–wave interactions for damage detection based on ultrasound—A review, *Journal of Sound and Vibration* **333**, pp. 1097-1118 (2014).

[33] Biwa, S., Nakajima, S. and Ohno, N., On the acoustic nonlinearity of solid-solid contact with pressure-dependent interface stiffness, *TRANSACTIONS-AMERICAN SOCIETY OF MECHANICAL ENGINEERS JOURNAL OF APPLIED MECHANICS* **71**, pp. 508-515 (2004).

[34] Ritdumrongkul, S. and Fujino, Y., Identification of the location and level of damage in multiple-bolted-joint structures by PZT actuator-sensors, *Journal of Structural Engineering* **132**, pp. 304-311 (2006).

[35] Amerini, F., Barbieri, E., Meo, M. and Polimeno, U., Detecting loosening/tightening of clamped structures using nonlinear vibration techniques, *Smart Materials and Structures* **19**, pp. 085013 (2010).

[36] Amerini, F. and Meo, M., Structural health monitoring of bolted joints using linear and nonlinear acoustic/ultrasound methods, *Structural Health Monitoring* **10**, pp. 659-672 (2011).

[37] Van Den Abeele, K. and Breazeale, M., Theoretical model to describe dispersive nonlinear properties of lead zirconate–titanate ceramics, *The Journal of the Acoustical Society of America* **99**, pp. 1430-1437 (1996).

[38] Meo, M., Amerini, F. and Amura, M., Baseline-free estimation of residual fatigue life using third order acoustic nonlinear parameter, *The Journal of the Acoustical Society of America* **4**, pp. 1829-1837 (2010).

[39] Arabian-Hoseynabadi, H., Oraee, H. and Tavner, P., Failure modes and effects analysis (FMEA) for wind turbines, *International Journal of Electrical Power & Energy Systems* **32**, pp. 817-824 (2010).